Effectiveness of systematic spike dithering depends on the precision of cortical synchronization

Antonio Pazienti[a,b,*], *Pedro E. Maldonado*[c], *Markus Diesmann*[d], *Sonja Grün*[d]

[a]*Neuroinformatics, Institute for Biology, Free University Berlin, Königin-Luise Street 1-3, 14195 Berlin, Germany*
[b]*Bernstein Center for Computational Neuroscience, Berlin, Germany*
[c]*CENI and P. Fisiología, Facultad de Medicina, Universidad de Chile, Casilla 70005, Santiago, Chile*
[d]*Theoretical Neuroscience Group, RIKEN Brain Science Institute, 2-1 Hirosawa, Wako-Shi, 351-0198 Japan*

A B S T R A C T

Spike synchronization is a candidate mechanism of cortical information processing. The widely used method of dithering randomly perturbs the spike times of experimental data to construct a distribution of coincidence counts enabling an assessment of the significance of the original data set. The precision of any existing synchrony, however, is limited by the biophysics of the neural system and detection methods are designed to tolerate an adjustable temporal spread. Previous works have independently studied the detectability of jittered spike coincidences and the destruction of precise coincidences by dithering. Here we derive for the first time how dithering interacts with temporally jittered coincidences. We demonstrate that the probability of detecting a spike coincidence characteristically decays with the applied dither interval. This unique relationship enables us to determine the precision of synchronization in cortical spike data of a freely viewing monkey based on the analysis for a single setting of tolerated temporal spread.

Keywords:
Synchronization
Spike dithering
Spike coincidence
Surrogate data
Visual cortex
Free viewing

1. Introduction

Current experimental protocols for the study of brain function result in highly non-stationary spike trains. In this context, experimental data typically contain a number of statistical features that do not allow an analytical treatment or parametric testing in particular in the context of the analysis of precise spike correlation of simultaneous spike trains. Therefore, surrogate methods are used to either implement the null-hypothesis for statistical tests or for additional controls. The idea behind such surrogate data sets is to destroy a particular feature, which we are interested to test for, while other features are preserved. In the context of spike correlation analysis, one aims to destroy spike correlation across the neurons while keeping features like the firing rate of the neurons, in time and across trials, and the internal spike train structure (i.e. to first order the inter-spike interval distribution) as similar as possible to the original data. Then these data are analyzed as the original data and compared to the latter. For this purpose a number of techniques for generating surrogates are used, like e.g. spike time randomization, trial shuffling, or modeling. However, each of them has some drawbacks in the sense that they involuntarily also destroy other features of the data that may lead to an uncontrolled perturbation of the data and may cause false positive results (Grün, submitted for publication).

In this context, spike dithering (Date et al., 1998) is currently considered as one of the best methods and widely used in correlation analysis (Abeles and Gat, 2001; Hatsopoulus

* *Corresponding author*. Neuroinformatics, Institute for Biology, Free University Berlin, Königin-Luise Street 1-3, 14195 Berlin, Germany. Fax: +49 30 83856686.
E-mail address: antonio.pazienti@neurobiologie.fu-berlin.de (A. Pazienti).

et al., 2003; Gerstein, 2004; Shmiel et al., 2006; Maldonado et al., submitted for publication). For doing so, each original individual spike is displaced randomly by a small amount to destroy the exact timing of the spikes but to conserve the trial by trial firing rates and the interval statistics of the data. Typically the randomization is undertaken homogeneously within a window around the spikes, but also other methods are in use that make the dithering dependent on the interval distributions to the foregoing and the following spike (Gerstein, 2004). In any case, the exact spike timing across the neurons is destroyed. However, depending on the allowed temporal scale of spike correlation, the dither range needs to be properly adjusted to reliably destroy the correlation features under evaluation. Pazienti et al. (2007) presented results on the destruction ability of dithering in a comparison of different coincidence detection methods. The limitation of the former study is that it only considers exact coincident events. The goal of this paper is to provide a theoretical understanding of the decay rate we have to expect if synchronous spike events of a given temporal jitter are present. Here we focus on (1) the usage of the multiple shift detection method for coincidence detection.We allow for (2) imprecise, "jittered" coincidences, which enables us to (3) explain effects of dithering observed in experimental data by relating them to underlying parameters. This is explored by simulations of stochastic point processes and confirmed by analytical derivations.

2. Results

2.1. *Detection of excess synchrony in experimental data*

In Maldonado et al. (submitted for publication) we investigated the neuronal activity in the visual cortex of monkeys while they freely view natural scenes (see Experimental procedures for details). The spike activity from small numbers of neurons and the eye movements were recorded simultaneously. The aim of the study was to not only investigate changes of discharge rate in individual neurons related to saccadic eye movements and the following fixation periods, but to examine correlations among simultaneously recorded spike trains. The hypothesis was that the early processing of visual information should not be based solely on rate coding but in addition on a temporal coding strategy in which the precise timing of individual spikes matters. During natural vision, processing times are so short that individual neurons can contribute only a few spikes to the computations required for scene segmentation and perceptual grouping. We found that right after the onset of fixation periods there is an excess of precise synchronous firing. These synchronizing events precede the transient and rather moderate rate increases that are observed after the onset of fixation (for suggested mechanisms see e.g. Fries et al., 2007). Fig. 1A (top panel, black curve) shows the averaged firing rate of 418 single units in response to fixations (data are triggered on fixation onset, i.e. time=0 ms) recorded in different sessions. The firing rate of the neurons (shown here by the average) starts to increase about 50 ms after fixation onset, reaches a maximum of about 15 Hz at 75 ms, and subsequently decays to base level again.

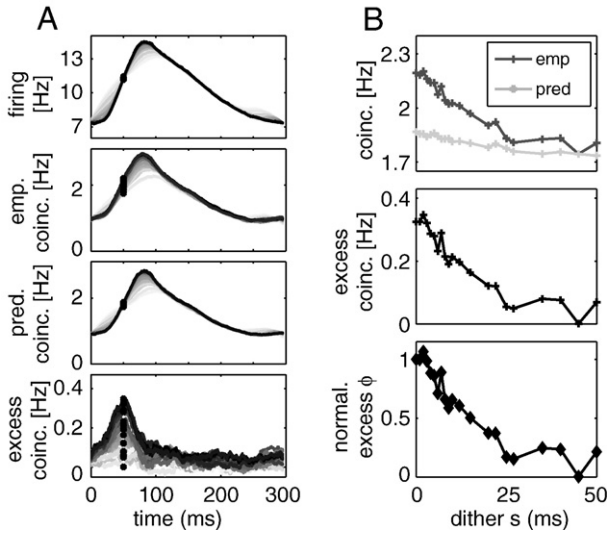

Fig. 1 – Dynamics of synchronization and the decay of excess coincidences with increasing dither width in experimental data. A: Synchronization dynamics modified from Maldonado et al. (submitted for publication). From top to bottom: firing rate, empirical, predicted, and excess coincidence rate. The data are averages over 1369 neuron pairs discretized with a resolution of δ=0.1 ms. The curves show results for different dither widths (black to light gray: s=0 to s=50 ms). The spike trains are dithered before the analysis is carried out in a sliding window of width 50 ms in steps of δ with a tolerated coincidence width of *b*=5 ms. The black asterisk at t=50 ms indicates the center of the data segment of 50 ms duration analyzed in the present study. B: The effect of dithering for the analysis window centered at the temporal position (t=50 ms) of the asterisk in A. The top panel shows the empirical and the predicted coincidence rate as a function of dither (same data as in A, second and third panel at asterisk, respectively). The middle panel shows the difference of the two measures (same data as in A bottom panel at asterisk). The bottom panel shows the same data as the middle panel normalized to the value at dither s=0.

For the analysis of correlated activity between neurons Maldonado et al. (submitted for publication) employed the unitary events analysis method (Grün et al., 2002a,b). This method is designed to detect coincident spike events and to evaluate their statistical significance in non-stationary settings. In the cited study, pairs of neurons are analyzed for the presence of significant excess synchronous activity, i.e. for empirical spike coincidences occurring significantly more often than predicted by the firing rates of the neurons. To allow a certain temporal imprecision of the coincident spike events, coincidences are detected by the multiple shift method (MS, Grün et al., 1999). Here, precise coincidences are counted (at the resolution δ of the data) by systematically shifting (up to ±*b*) the second spike train with respect to the first. Consequently, spikes with a distance of up to ±*b* bins are counted as coincident. The total sum of all detected coincidences over all shifts is the empirical number of coincidences n_{emp}. The synchronization between pairs of spike trains is quantified by the number of coincidences exceeding the predicted number n_{pred} assuming independence. The latter is

calculated based on the product of the firing probabilities of the neurons multiplied by the number of bins T. The number of excess coincidences is then simply the difference between the empirical and the predicted counts, i.e. $n_{exc}=n_{emp}-n_{pred}$. In a situation where results are averaged over trials or across different neurons pairs the measures are expressed as empirical λ_{emp}, predicted λ_{pred}, and excess coincidence rate λ_{exc}, respectively.

In order to account for changes in the firing rates in time, the outlined analysis is performed in a sliding window fashion (here: box car of 50 ms width) yielding time resolved results. The results of the latter performed for all 1369 pairs of neurons are shown in Fig. 1A as averaged coincidence rates (second panel from top: empirical coincidence rates; third panel: predicted coincidence rates).

The time course of the excess synchrony, i.e. empirical coincidence rate reduced by the predicted coincidence rate (for each pair, then averaged) is shown in the bottom panel. Maldonado et al. (submitted for publication) showed that this increase of excess synchrony around 50 ms after fixation onset is highly significant and is manifested by the occurrence of unitary events (not shown here).

To demonstrate that the occurrence of excess synchrony is not a false positive effect induced by the non-stationarity in the firing rates, additional controls were performed. One is to intentionally destroy the spike synchrony while preserving the firing rates of the neurons. If excess synchrony is the origin of the peak in the measured excess synchrony, this peak should disappear. Therefore spike dithering was employed: Each individual spike is randomly and uniformly relocated within a small time window centered at the original spike time (in the range $\pm s$ in units of δ). This is applied independently to all spikes of both neurons ("2-neuron dithering", Pazienti et al., 2007). Fig. 1A (bottom panel) illustrates how dithering, performed for increasing dither width s up to ±50 ms, leads to a systematic decay of excess synchrony. The amplitude at 50 ms after fixation onset decreases with increasing dither, while the firing rate is only moderately smoothed (Fig. 1A, top).

Fig. 1B depicts the situation at the time of maximal excess synchrony (i.e. at 50 ms, indicated by asterisks in Fig. 1A). The predicted coincidence rate λ_{pred} stays approximately constant for increasing dither widths, while the empirical coincidence rate λ_{emp} decays (Fig. 1B, top panel). As a consequence, also the excess synchrony decays (Fig. 1B, middle panel). This can also be expressed as the normalized excess $\phi(s)$ by dividing the difference of the empirical and the predicted rate at a given dither width s by the original excess value: $\phi(s)=\frac{\lambda_{emp}(s)-\lambda_{pred}(s)}{\lambda_{emp}(s=0)-\lambda_{pred}(s=0)}$ (Fig. 1B, bottom panel).

Since the speed of the decay appears slow, one may still argue that it is actually due to the flattening of the firing rate profile induced by the dithering. In the course of this paper we provide a theoretical understanding of the speed of the decay of excess synchrony in the presence of coincident spike events with temporal jitter. As a result we confirm that the observed decay in our experimental data is not due to a perturbation of the rate profile.

2.2. *Stochastic model and simulation*

We simulate two parallel point processes modeling the spiking activity of the neurons. The processes have identical firing rate λ (in Hz) and contain a variable degree of correlation. The spike trains are generated in two steps. In the first step we insert spikes into T/δ successive bins of width δ independently for each neuron (background firing). The spike times are obtained from Poisson processes of background rate λ_b. In the second step, we draw a single train of spike times from a Poisson process of rate λ_c. These spike times are inserted into the background spike train of the first neuron. However, in order to describe a certain natural temporal jitter of the spikes constituting a coincidence, before insertion into the spike train of the second neuron each spike is randomly displaced within a window $[-j, j]$ with uniform probability around the original position ("jittering", Grün et al., 1999). Clipping is applied to avoid multiple spikes in the same bin. The total rate of both neurons is approximately the sum of the background and the correlated firing rate.

2.3. *Analytical description of excess synchrony*

The predicted number of coincidences between two processes having background and coincidence rates λ_b and λ_c respectively equals $(\lambda_b\delta+\lambda_c\delta-\lambda_b\lambda_c\delta^2)^2\,T$. The third term of the spike probability accounts for the reduction in spike rate due to the clipping process (see Grün et al., 1999). When using the MS method for coincidence detection each of the $2\cdot b+1$ shifts contributes the same number of predicted coincidences. This yields (Grün et al., 1999) a total of

$$n_{pred}(b,\lambda_b,\lambda_c,\delta,T)=(2b+1)\left(\lambda_b\delta+\lambda_c\delta-\lambda_b\lambda_c\delta^2\right)^2T. \quad (1)$$

The empirical number of coincidences after dithering is the sum of two terms $n_{emp}=n_{emp,c}+n_{emp,r}$. The first term is given by the fraction of inserted coincidences that are detected by the MS method, $n_{emp,c}$. This term depends on the amount of jitter j, of the dither s, and of the performed number of shifts specified by the parameter b. The second term is given by the number of "background coincidences" $n_{emp,r}$.

The number of injected coincidences that are detected can be expressed as the total number of injected coincidences times the probability of detection, i.e. $n_{emp,c}=P^{[MS_j]}(s,b,j)\cdot\lambda_c\delta T$. In a previous work we calculated the probability of detection for the case of no jitter (Pazienti et al., 2007). Here we extend this result and include in our analysis the presence of jittered coincidences. To obtain the probability of detection $P^{[MS_j]}(s,b,j)$ we sum the corresponding probabilities for all jitters from $-j$ to j:

$$P^{[MS_j]}(s,b,j)=\frac{1}{2j+1}\sum_{i=-j}^{j}P_i^{[MS_j]}(s,b).$$

Following the approach of Pazienti et al. (2007), Sec. 3, we obtain the probability that the spikes of an exact coincidence after dithering have a distance k as $J(s,k,j)=\frac{1}{2s+1}\sum_{d=-s}^{s}p(k+d)$, where $p(k+d)$ is the probability that the spike of neuron 2 is in distance k from the spike of neuron 1 at position d. Due to the jitter j, the possible relative positions of the two spikes are subject to a number of constraints. When applying the MS method the number of performed shifts to the left and to the right, b_L, b_R, resulting in non-zero contributions now depend on the variables s, b, and j. In particular, the initial jitter

introduces an asymmetry for the MS method. For example, if spike 2 is to the right of spike 1 ($j>0$) it is more likely that after dithering the distance k between the two spikes is still positive. Furthermore, the maximal distance between two jittered spikes after dithering is $2s+|j|$. Thus with a MS-parameter $b \geq 2s+|j|$ all coincidences are detected. The number of shifts to be considered to the left and to the right are

$$b_L(j) = \begin{cases} \min(2s-|j|, b) & \text{for } j \geq 0 \\ \min(2s+|j|, b) & \text{for } j < 0 \end{cases}$$

and

$$b_R(j) = \begin{cases} \min(2s+|j|, b) & \text{for } j \geq 0 \\ \min(2s-|j|, b) & \text{for } j \geq 0 \end{cases}$$

This yields for the probability of detection at a given jitter position i:

$$P_i^{[MS_j]}(s,b) = \sum_{k=-b_L(i)}^{b_R(i)} J(s,k,i) = \sum_{k=-b_L(i)}^{b_R(i)} \frac{2s+1-|k-i|}{(2s+1)^2}$$

$$= \begin{cases} 1 & ,b \geq 2s+|i| \\ \frac{2b+1}{2s+1} - \frac{b(b+1)+i^2}{(2s+1)^2} & ,|i| \leq b \leq 2s-|i| \\ \frac{2b+1}{2s+1} - \frac{(2b+1)\cdot|i|}{(2s+1)^2} & ,|i| \geq b, b \leq 2s-|i| \\ \frac{1}{2} + \frac{1+2(b-|i|)}{2(2s+1)} - |b-|i|| \cdot \frac{b-|i|+1}{2(2s+1)^2} & ,2s-|i| \leq b \leq 2s+|i| \\ 0 & ,b < |i|-2s \end{cases} \quad (2)$$

Next we need to compute the number of coincidences contributed by the background $n_{emp,r}$. Grün et al. (1999) showed that these coincidences are composed of spikes originating from the original background rate and of debris of undetected injected coincidences. Considering the additional dithering of spikes the expression reads

$$n_{emp,r} = \begin{cases} \sum_{k=-b}^{b} \left[\lambda_b \delta - \lambda_b \lambda_c \delta^2 + \lambda_c \delta (1 - P_k(k))\right]^2 T & ,b \leq 2s+j \\ \sum_{k=-(2s+j)}^{(2s+j)} \left[\lambda_b \delta - \lambda_b \lambda_c \delta^2 + \lambda_c \delta (1 - P_k(k))\right]^2 T & \\ + \left(\lambda_b \delta - \lambda_b \lambda_c \delta^2 + \lambda_c \delta\right)^2 [(2b+1) - (2(2s+j)+1)] T & ,b > 2s+j \end{cases} \quad (3)$$

If b does not exceed the range over which originally coincident spikes are spread out due to the jitter and the subsequent dithering, only the fraction $1-P_k(k)$ of undetected spikes from coincidences (debris) contribute to $n_{emp,r}$. k is the current shift of the MS procedure. Additional spike probability is caused by the background spikes corrected for the loss $\lambda_b \lambda_c \delta^2$ due to clipping. If b exceeds the critical range, $n_{emp,r}$ decomposes into two terms. Up to the maximum shift $2s+j$ where originally coincident spikes can still become coincident again only debris contribute to the background. For larger shifts originally coincident spikes contribute to the background with the unreduced probability $\lambda_c \delta$. Note that in the absence of dither ($s=0$) the expression for $n_{emp,r}$ is the same as Eq. 18 in Grün et al. (1999). In this situation the probability of detection $P_k(k)$ only depends on the jitter range and takes the form $1/(2j+1)$. After dithering the probability is $P_k(k) = \sum_{i=-s}^{s} f_1(i) f_2(i+k)$ with $f_{1/2}(i)$ being the probability to find a spike of an injected coincidence at relative position i for neuron 1 and neuron 2, respectively. Because the jitter is only applied to neuron 2 we have

$$f_1(i) = \begin{cases} \frac{1}{2s+1} & ,|i| \leq s \\ 0 & ,i > 0 \end{cases}$$

and

$$f_2(i) = \begin{cases} \frac{1}{2\max(s,j)+1} & ,|i| \leq |s-j| \\ \frac{1}{2s+1}\frac{1}{2j+1}(1+s+j-|i|) & ,|s-j| < |i| \leq s+j \\ 0 & ,|i| > s+j \end{cases}$$

Using Eqs. (1), (2) and (3) we can now write the number of excess coincidences as

$$n_{exc}(s,b,j;\lambda_b,\lambda_c) = n_{emp,c} + n_{emp,r} - n_{pred} \quad (4)$$

and the normalized excess as

$$\phi = \frac{n_{exc}(s,b,j,\lambda_b,\lambda_c)}{n_{exc}(s=0,b,j,\lambda_b,\lambda_c)}. \quad (5)$$

The latter measure can be interpreted as the probability to detect a coincidence after dithering. Thus, we have derived a relationship between the five parameters determining the observation of excess synchrony: s, b, j, λ_b, λ_c.

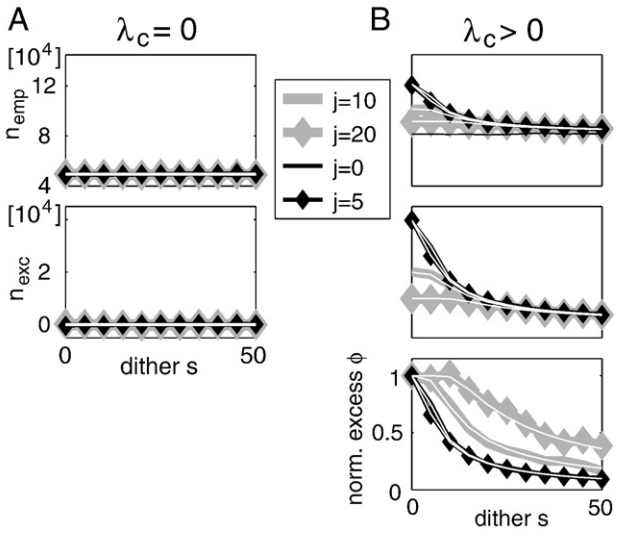

Fig. 2 – Decrease in excess coincidences as a function of dither in simulations of a stochastic model (black and gray) and analytical descriptions (white) A: Without injected coincidences at background activity $\lambda_b = 35$ Hz for $T \cdot \delta = 10$ ms with resolution $\delta = 0.1$ ms. Analysis carried out with tolerated coincidence width $b = 5$ ms. The different curves (black and gray) show results for different realizations of the stochastic process and different temporal jitter of coincidences (see legend, specified in ms, but no coincidences here). Top: empirical coincidences, middle: excess coincidences. B: Same as A with coincidences injected at rate $\lambda_c = 10$ Hz. Additional bottom panel: normalized excess coincidences. The speed of decay depends on the jitter of the coincidences, compare to experimental results in Fig. 1B. The black horizontal line in the top panel indicates the predicted number of coincidences.

2.4. *Presence of coincidences shapes the decay*

When no coincidences are inserted (i.e. $\lambda_c = 0$) the empirical number of coincidences equals the number predicted by the firing rates. The top panel of Fig. 2A illustrates that the empirical coincidence count n_{emp} does not depend on the dither s. The same is true for the predicted number of coincidences n_{pred} (not shown). Therefore, the number of excess coincidences n_{exc} (Fig. 2A bottom panel) is zero for all dithers. In this situation the normalized number of excess coincidences ϕ (Eq. (5)) is undefined.

A different scenario arises when the neurons are correlated, i.e. $\lambda_c > 0$, as shown in Fig. 2B. The empirical coincidence count now exceeds the predicted value (top panel, black thin horizontal line). The empirical number of coincidences converges to the predicted number with increasing dither, thus the excess coincidence count converges to 0 (middle panel). Correspondingly, the normalized excess coincidences ϕ also decreases with increasing dither (bottom panel). The experimental data in Fig. 1B exhibit a similar behavior: The empirical coincidence rate slowly converges to the predicted one for increasing dither, such that the excess coincidence rate almost decays to 0. As a consequence, also the normalized excess coincidences ϕ decay from 1 to very low values.

In the simulated data we can additionally observe how these measures behave for various degrees of the temporal jitter j of coincidences, represented in Fig. 2 by different gray values and line markers. j assumes the values 0, 5, 10, and 20, while the parameter for detection ($b = 5$) is fixed. For jitter values up to the value of the allowed coincidence width b the graphs for ϕ coincide (black curves without marker and with diamonds, Fig. 2B, bottom panel). For larger values of the jitter j, ϕ decays more slowly (gray curves). For $j > b$ (black curves), all coincidences are detected for small jitter, but for increasing dither the spikes are rapidly scattered out of the detection window, and therefore ϕ, decays fast. On the contrary, for $j > b$, there is no chance to detect all coincidences, thus n_{exc} starts at smaller values, and decays less. This is reflected in the slow decay of ϕ since already at small dithers the coincidence count is close to the predicted level. Note the perfect agreement of the simulation results and the analytical descriptions (white curves).

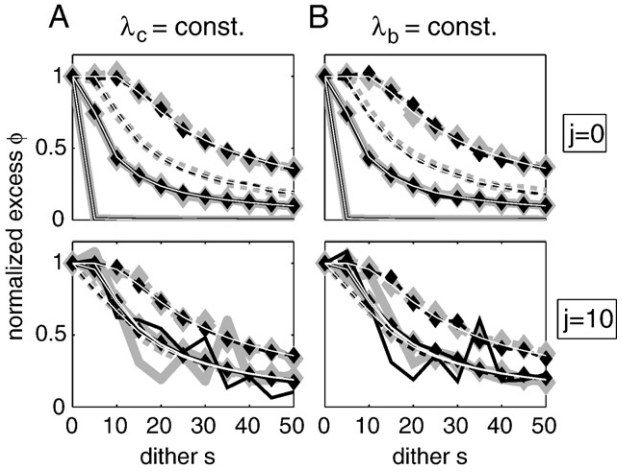

Fig. 3 – Effect of spike rates on the normalized excess coincidences as a function of dither. A: Fixed coincidence rate ($\lambda_c = 5$ Hz) and two levels of background rate $\lambda_b = 5$ Hz (black) and 25 Hz (gray). B: Fixed background rate ($\lambda_b = 25$ Hz) and two levels of coincidence rate $\lambda_c = 5$ Hz (black), 10 Hz (gray). In all panels the analysis is carried out for a range of tolerated coincidence width: $b = 0$ ms (solid), 5 ms (solid with diamonds), 10 ms (dashed), and $b = 20$ ms (dashed with diamonds). The top row shows the results for perfect coincidences ($j = 0$ ms), the bottom row for a jitter of 10 ms. Analytical results for all cases are shown in white.

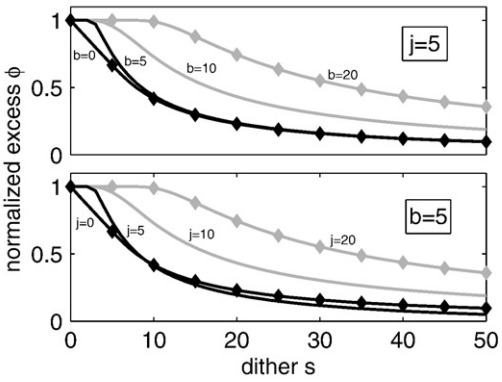

Fig. 4 – Symmetry of temporal jitter and tolerated coincidence width. The top panel shows the decay of the normalized excess coincidences as a function of dither for a fixed temporal jitter ($j = 5$ ms) and tolerated coincidence width $b = 0$ ms (black with diamonds), 5 ms (black), 10 ms (gray), 20 ms (gray with diamonds). In the bottom panel the parameterization of j and b is exactly reversed. All curves show analytical results, computed in the absence of background activity $\lambda_b = 0$ Hz, $\lambda_c = 5$ Hz, $T \cdot \delta = 10^6$ ms, and $\delta = 0.1$ ms.

2.5. *Independence from rates*

Next we are interested in the decay of the normalized excess coincidences ϕ as a function of rate levels, i.e. background firing rate and coincidence rate. Therefore we analyze simulated data for ϕ for various detection parameters b (0, 5, 10, 20, i.e. different graphs with identical gray values in each panel). Additionally we vary the background firing rate λ_b (Fig. 3A, black: 5 Hz, gray: 25 Hz) and in Fig. 3B the coincidence rate λ_c (black: 5 Hz, gray: 10 Hz). Clearly, the graphs for different firing rates within the single panels are in agreement, indicating that ϕ is not affected by rates. The non-normalized excess coincidences are slightly different for different background rates (not shown), but the normalization procedure causes these differences to cancel out. This holds true for any value of the parameters j, b, s, as shown for the simulations as well as for the analytical results (thin white curves). Therefore the background rate may be neglected for considerations of the normalized excess coincidences ϕ.

2.6. *Symmetry of jitter and shift*

Fig. 4 shows the analytical results for the normalized number of excess coincidences as a function of the variables s, b, j. For

the reasons discussed above, we here neglect the background rate (i.e. $\lambda_b=0$). As shown above, ϕ decays as a function of increasing dither s, since coincidences are more and more destroyed and their detectability becomes lower and lower at constant b. If the jitter value j is kept constant while increasing the MS-parameter b, the decay of the excess coincidences gets slower (top panel). An analogous scenario is observed when keeping b constant and increasing the jitter j (bottom panel). The two panels of Fig. 4 display a very similar behavior for simultaneous variations of the variables b and j. Indeed, we observe two types of symmetry: 1) the overall behavior of ϕ as a function of s and combinations of the values of j and b is similar (cf. top and bottom panels); 2) for j fixed and $b \leq j$ and vice versa the curves overlap (black curves on both panels and see also Fig. 3, bottom panels). This symmetry in the effect of b and j on ϕ is, however, due to two different reasons.

On the one hand, when keeping b constant and varying j for increasing dither Eq. (2) is dominated by the term $(2b+1)/(2s+1)$ (first part of the second and third terms on the right side of Eq. (2)), which is independent of j. Thus the probability $P^{[MS_j]}(s,b,j)$ converges to the same asymptotic value for any j. Furthermore, for $s=0$ and $b>j$ all coincidences are detected. These two facts explain why the excess coincidences agree for any $j \leq b$ (Fig. 4, bottom panel, black curves). However, if $j>b$ the value of the probability at $s=0$ is smaller than 1, and the normalization leads to a slower decay of detection rate (gray curves).

When on the other hand j is kept constant and b is varied (Fig. 4, top panel), the probability $P^{[MS_j]}(s,b,j)$ critically depends on b, and increases as b is increased (not shown). However, in this case both the empirical and the predicted number of coincidences in Eq. (3) scale with the factor $(2b+1)$. For $b>j$ some amount of dither is required for effective destruction of coincidences.

2.7. *Agreement with experimental results*

Let us compare the theoretical prediction of the effect of dithering on excess coincidences with the experimental data. The experimental results are obtained for $b=5$, therefore we fix this parameter also for the theoretical considerations. The excess coincidence rate is obtained from Fig. 1B, middle panel, at $s=0$ as $\lambda_{exc}=0.32$ Hz and interpreted as the rate of injected coincidences λ_c while employing the arguments of section 2.5, the background rate λ_b is assumed to be zero. In order to fit the model to the experimental data we are left with one open parameter, i.e. the jitter j. Fig. 5 shows the theoretical decay probability for a range of j from 5 to 10 ms (gray area). The experimental data points are marked by crosses along the thick dashed curve within an envelope of ±1 standard deviation (thin dashed curves). The white curve shows a good overall fit to the experimental data for $j=7$ ms. The observation that the experimental curve is systematically below the theoretical prediction for large dithers is due to the non-stationarity in the firing rate profile around the time point of evaluation (cf. Fig. 1A, black asterisks). The reason is that the predicted coincidence rate slightly decreases for increasing dither (Fig. 1B, top panel) due to an unbalance of spikes dithered out and into the analysis window near the left border of the analysis window (not shown). This effect becomes only noticeable at extremely large dither ranges. Further work should explore whether dithering methods conserving the rate profile can be constructed.

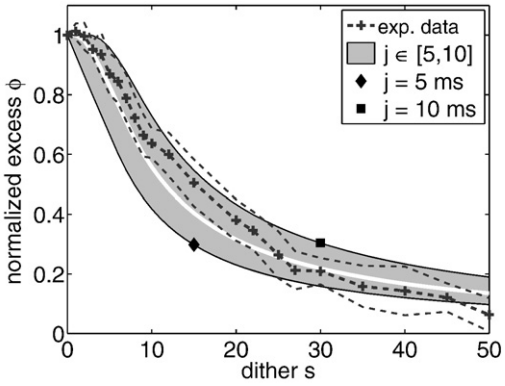

Fig. 5 – Comparison of experimental data and model results. The dashed curve marked with crosses shows experimental data. In contrast to Fig. 1B bottom panel here we show the average of 16 repetitions of dithering of the experimental data in the corresponding envelope (thin dashed curve) of one standard deviation. The gray band is enclosed by theoretical results for a temporal jitter of $j=5$ ms (diamond) and $j=10$ ms (square). An intermediate value of $j=7$ ms is indicated by the solid white curve. Experimental and model results are computed for a tolerated coincidence width of $b=5$ ms at a resolution of $\delta=0.1$ ms. The remaining model parameters are: $\lambda_b=0$ Hz, $\lambda_c=0.32$ Hz, $T\cdot\delta=10^6$ ms.

In summary, the comparison of the theoretical results and the experimental data demonstrates that the observed decay of excess coincidences is quite well predicted by our model and indicates a temporal jitter in the experimental data of about ±7 ms. The fact that the excess coincidences exhibit a characteristic decay with increasing dither proves the existence of excess synchrony, which cannot be explained by rate effects.

3. Discussion

The study of Maldonado et al. (submitted for publication) revealed the presence of spike synchrony in early visual processing of freely viewing monkeys. The authors demonstrated that the significance deteriorates if the experimental spike data are intentionally dithered and that the dependence on dither width is consistent with simulations of jittered coincidences embedded in uncorrelated background spikes. The slowness of the decay, however, remained a puzzle. As large dithers have undesired side effects like flattening of the rate profile, destroying the spike train structure, and scattering of spikes out of the analysis window understanding the mechanism of coincidence fission gained some priority. First insights came from Pazienti et al. (2007). Considering isolated precise coincidences the authors derive analytical expressions for the dependence of the number of surviving coincidence as a function of the dither width. The results confirmed the slowness of the decay.

However, the strong assumptions of this model are clearly violated by the experimental data which is immediately raising the question whether the natural temporal spread renders coincidences more sensitive to dithering. In contrast, the presence of background activity may interfere with the effectiveness of dithering. The work of Grün et al. (1999) provides an analytical framework for handling the various interaction terms but is limited to the case without dithering. In the present work we have combined the results of Grün et al. (1999) and Pazienti et al. (2007) to arrive at an analytical description containing all three parameters: jitter, dither width, and tolerated coincidence width. Unlike the earlier study by Grün et al. (1999) we do not study the significance of the coincidences but for clarity limit the discussion to the probability of a coincidence to survive the dithering process. In the physiological parameter range our measure is insensitive to the values of background activity λ_b and coincidence rate λ_c. This leaves us with only one free parameter of the model: the natural jitter of the coincidences.

Our results show that the jitter is constraint to a quite narrow range of a few milliseconds around a good general fit for a jitter of $j=7$ ms. Our earlier work on data from motor cortex (Grün et al., 1999) arrived at a value of $j=6$ ms. At large dithers the variability of our measure increases due to the low number of surviving coincidences. Consequently, the jitter is less constraint than at small dithers. The choice of a uniformly distributed jitter in spike synchrony is not motivated by biophysical considerations but by computational convenience only. Presumably a better fit to the characteristic decay of survival probability can be obtained with a more realistic assumption about the shape of the spike jitter. The data exhibit a considerably larger survival probability than predicted by the model in a certain interval around a dither width of 15 ms. This may indicate that the data exhibit more than one time-scale of synchronization. Future work needs to incorporate the significance of the surviving coincidences again. Using this measure not only spike jitter but also the background and the coincidence rate can be estimated. The number of surviving coincidences, and thus significance, characteristically depends on both parameters of the analysis, tolerated coincidence width (Grün et al., 1999) and dither width (this work). A two-dimensional analysis of significance therefore potentially reveals further details of the temporal structure of the spike jitter. A major constrained of the analysis presented here is that larger dithers destroy more of the individual spike train structure and the rate profile. Gerstein (2004) has recently developed a dither method, which better conserves the inter-spike-interval distribution. We need to investigate whether the lower limit for the dither width resulting from our studies is compatible with the desire to conserve essential features of the spike train structure.

4. Experimental procedures

4.1. *Neurophysiological data*

Spike trains of simultaneously recorded neurons were obtained from the primary visual cortex of two adult capuchin monkeys (*Cebus apella*). Full details of these recordings can be found in Maldonado et al. (submitted for publication). All experiments followed institutional and NIH guidelines for the care and use of laboratory animals. Briefly, animals seated in a dimly lit chamber were allowed to freely explore 15 different natural images presented on a 21-in. computer monitor located 57 cm in front of the animals, subtending 30×40° of visual angle. The experimental protocol required the animals to maintain their gaze for up to 5 s within the limits of the images, to be rewarded with a drop of juice. Vertical and horizontal eye positions were monitored with a search coil driver (DNI Instruments). Neuronal activity of neighboring neurons was recorded with an array of 8 individually adjustable tetrodes (1–2 MΩ impedance). The signals were amplified (10 K), band pass filtered for single unit activity (0.5 kHz–5 kHz), sampled at 25 KHz and then stored for off-line spike sorting and analysis. Signals were fed through an off-line sorting program to reconstruct the spike trains of units recorded simultaneously by each single tetrode (Gray et al., 1995). An automatic algorithm was developed to extract saccades (angular velocity higher than 100°/s) and visual fixations consisting in visual position maintained for at least 100 ms, within 1° of the gaze location reached at the end of a saccade. For subsequent analysis of neuronal activity, each individual visual fixation is referred as a "trial" and the measurement period during which electrode positions were kept constant and the constellation of recorded cells was stable as "recording session". Trials of fixations were analyzed individually and subsequently those occurring during different images presentations and within the same recording session were grouped.

Acknowledgments

Partly funded by Stifterverband für die deutsche Wissenschaft, the Bernstein Center for Computational Neuroscience Berlin (BMBF grant 01GQ014123), the Iniciativa Cientifica Milenio P04-068F, and DIP F1.2.

REFERENCES

Abeles, M., Gat, I., 2001. Detecting precise firing sequences in experimental data. J. Neurosci. Meth. 107, 141–154.

Date, A., Bienenstock, E., Geman, S., 1998. On the temporal resolution of neural activity. Technical report, Division of Applied Mathematics. Brown Univ. (available at http://www.dam.brown.edu/people/elie/papers/temp-res.ps).

Gerstein, G.L., 2004. Searching for significance in spatio-temporal firing patterns. Acta Neurobiol. Exp. (Wars) 64, 203–207.

Fries, P., Nikolić, D., Singer, W., 2007. The gamma cycle. Trends Neurosci. 30 (7), 309–316.

Gray, C.M., Maldonado, P.E., Wilson, M., McNaughton, B., 1995. Tetrodes markedly improve the reliability and yield of multiple single-unit isolation from multi-unit recordings in cat striate cortex. J. Neurosci. Methods 63, 43–54.

Grün, S., submitted for publication. Data driven significance estimation of precise spike synchronization.

Grün, S., Diesmann, M., Grammont, F., Riehle, A., Aertsen, A., 1999. Detecting unitary events without discretization of time. J. Neurosci. Meth. 94, 67–79.

Grün, S., Diesmann, M., Aertsen, A., 2002a. 'Unitary Events' in multiple single-neuron activity. I. Detection and significance. Neural Comput. 14, 43–80.

Grün, S., Diesmann, M., Aertsen, A., 2002b. 'Unitary Events' in multiple single-neuron activity. II. Non- Stationary data. Neural Comput. 14, 81–119.

Hatsopoulus, N., Geman, S., Amarasingham, A., Bienenstock, E., 2003. At what time scale does the nervous system operate? Neurocomputing 25–29 52–54.

Maldonado, P., Babul, C., Singer, W., Rodriguez, E., Berger, D., Grün, S., submitted for publication. Dissociation between neuronal discharge rates and synchrony in primary visual cortex of monkeys viewing natural images.

Pazienti, A., Diesmann, M., Grün, S., 2007. Bounds of the ability to destroy precise coincidences by spike dithering. Lecture Notes in Computer Science 4729, 428–437.

Shmiel, T., Drori, R., Shmiel, O., Ben-Shaul, Y., Nadasdy, Z., Shemesh, M., Teicher, M., Abeles, M., 2006. Temporally precise cortical firing patterns are associated with distinct action segments. J. Neurophysiol. 96 (5), 2645–2652.